

Tailoring superhydrophobic surfaces on AA6082 aluminum alloy by etching in HF/HCl solution for enhanced corrosion protection

A. Khaskhoussi, L. Calabrese, E. Proverbio

The most important challenge in the shipbuilding is the weight reduction of the naval structures traditionally made of steel in order to increase their stability and safety. Aluminum and its alloys are potential candidate materials thanks to their lightweight and excellent weldability. However, aluminum alloys are prone to pitting corrosion in saline environment. Controlling the water repellency of aluminum surface can provide passive solution to protect it. Herein, the effect of chemical etching on the surface morphology and the anti-wetting behavior of AA6082 alloy, after hydrophobic treatment in a silane/toluene solution, were assessed. Indeed, different etching times were considered to optimize the treatment effect. The results indicate that the prepared surfaces reached the threshold value for superhydrophobicity (150°). However, the contact and sliding angles strongly depend on the etching time. Optimized superhydrophobic surfaces achieved an enhanced corrosion protection compared to the as-received AA6082 in simulated seawater.

KEYWORDS: SUPERHYDROPHOBICITY; ALUMINUM ALLOY; CORROSION; CHEMICAL ETCHING;

INTRODUCTION

In recent years, inspired by lotus leaves effect, artificial superhydrophobic surfaces have attracted extensively attention. A surface with a contact angle (CA) higher than 150° and a sliding angle (SA) lower than 10° with water is well-defined as a superhydrophobic surface. Research has revealed that this surface shows a great potential for various applications such as anticorrosion [1,2], self-cleaning [3], oil-water separation [4], anti-icing [5]. Presently, there are several methods to fabricate superhydrophobic surfaces, sol-gel [6], electrodeposition [7], vapor deposition [8], laser etching [9], etc. These techniques aim to construct rough structures and low surface energy on the substrate surface, which are both necessary conditions for the surface to become superhydrophobic.

Due to its low density, elevated electrical conductivity, adequate mechanical strength, oxidation resistance, and low cost, aluminum alloys have been widely used in nu-

**Amani Khaskhoussi, Luigi Calabrese,
Edoardo Proverbio**

Department of Engineering, University of Messina; Messina, Italy

akhashoussi@unime.it,
lcalabrese@unime.it, eproverbio@unime.it

merous fields, such as shipbuilding, automobile, construction, mechanical equipment [10]. Thanks to the large-scale use of this metal, their application scenarios are variable. For numerous aluminum products and equipment working in high humidity, dirty, and low temperature, the accumulation of water, snow, and dirt on its surface can limit the operation of the equipment or even destroy it [11]. For this reason, it is necessary to improve the anti-corrosion, anti-icing, water repellence performances of the aluminium surfaces.

The chemical etching can be used to fabricate superhydrophobic surfaces because of its efficiency, simplicity and low cost in obtaining a tailored rough surface. Indeed, aluminum and its alloys are reactive metals that can easily react with strong acids to etch out coarse surface microstructures. The adjustment of the etching conditions can be an effective method to create hierarchical nano-micro structure that is necessary to reach the desired superhydrophobicity.

In the present work, superhydrophobic surfaces were created on aluminum alloy following a simple two-steps method. Nano/Micro structures were fabricated by acid etching, at different times, and the free energy of the surface was reduced using a thin silane film. Then, the wetting behavior was investigated. In addition, the effect of the etching time on the corrosion performances of the superhydrophobic aluminum surfaces have been studied.

MATERIALS AND METHODS

Aluminium alloy plates EN AW-6082 T6 were cut into 30×24×2 mm pieces followed by cleaning with ethanol and acetone in an ultrasonic bath for 5 min. Hydrochloric acid (37 wt%), distilled water and HF (48 wt%) are prepared in a 15:4:1 vol ratio to make a mixed acid solution. Each sample, with the as received surface, was etched in the same 50 ml of the mixed acid solution for 5, 15 and 30s, followed by cleaning in an ultrasonic bath with ultra-pure water for 2 min. Afterward, the samples were blown dry and soaked in 1 vol% silane toluene solution for 10 min. Finally, the samples were cured in a constant temperature drying oven at 100 °C for 3 h.

The static water contact angles on the sample surface were measured, at room temperature, using an Attention Theta Tensiometer by Biolin Scientific according to the sessile drop technique. Ten replicas of water contact angle (CA) and water sliding angle (SA) for each sample were made. Morphological analysis of the prepared surfaces was performed using the scanning electron microscope (SEM, ZEISS Crossbeam 540). Roughness parameters of the surfaces were calculated based on the profiles analysis using the Mitutoyo profilometer SJ-210 (Japan). Electrochemical measurements were carried out, in simulated seawater electrolyte (3.5 wt.% NaCl solution) at room temperature, using a BioLogicSP-300 potentiostat. A standard three-electrode cell composed by a saturated Ag/AgCl electrode as the reference electrode, a platinum wire as the counter electrode, and the prepared aluminium sample as the working electrode (exposed area = 1cm²), was utilized as the working cell. After reaching the OCP, the EIS test was performed with a voltage amplitude of 10 mV and a frequency range from 0.5 Hz to 10⁵ Hz.

RESULT AND DISCUSSION

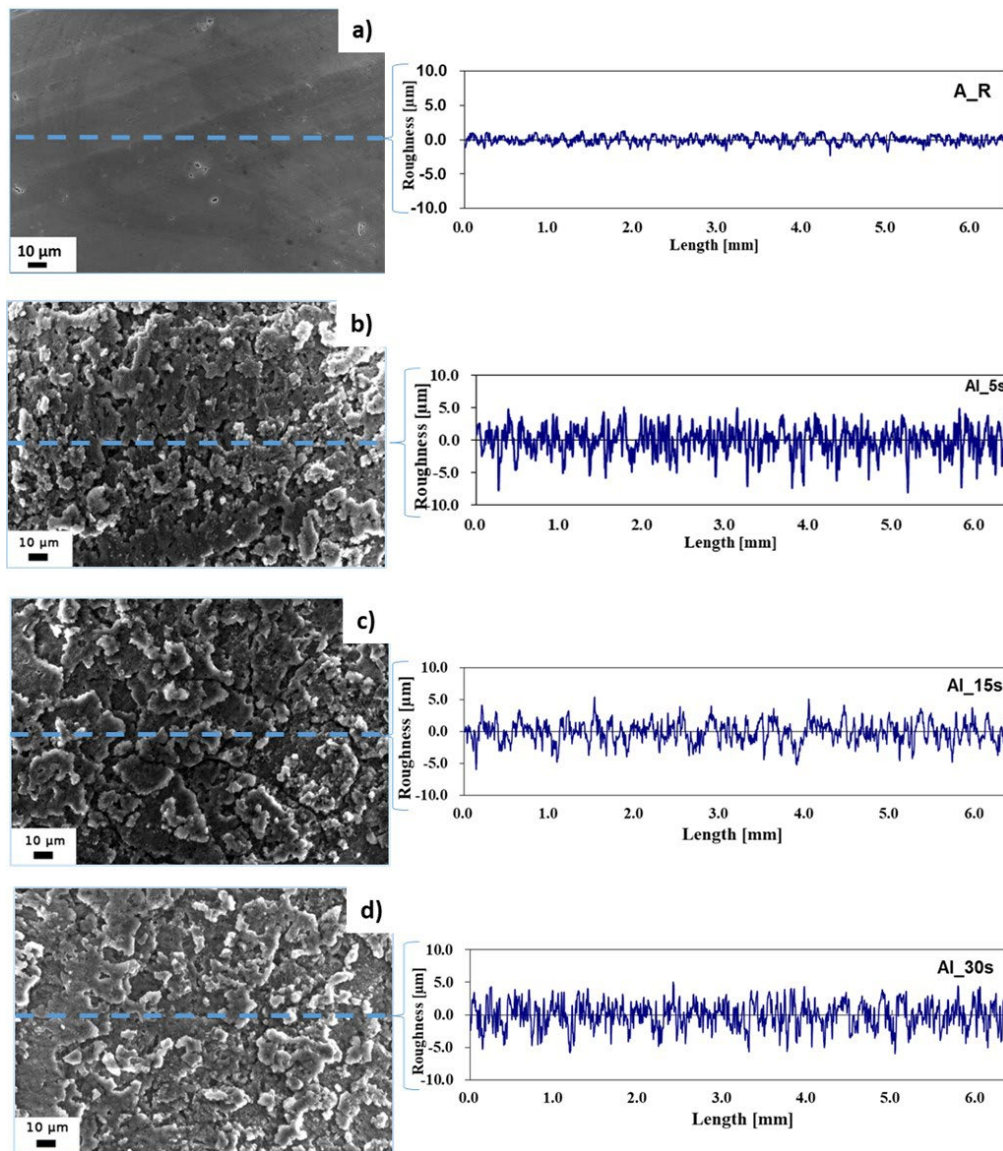


Fig.1 - Surface morphologies of the as received surface (a), etched surfaces for 5s (b), 15s (c) and 30s (d) in original magnification of 5 kX

Fig. 1 illustrates the SEM images and the roughness profiles of the AA 6082 surfaces at different etching times. It can be seen that the treatment of the AA 6082 substrates with HF/HCl etchant for different of times influence the surface morphology of the as-received aluminium substrates from a flat toward a hierarchical rough surface. After 5 seconds of etching, micrometer-sized rough structure was formed like a coral network. At increasing etching time to 15s, the coral network microstructure is still preserved and becomes more homogeneous and regular with quite similar sequence of peaks and valleys as shown in the sur-

face profile (Fig.1.c). Then, at longer etching time (30s), the aluminium surface appears rough but begins to slightly lose the sequence order of peaks and valleys (Fig. 1.d).

These microstructures are a consequence of the intrinsic substrate heterogeneity. Indeed, the aluminium alloy has a large number of dislocations, defects and microstructural heterogeneities. These local defects are more reactive than other substrate areas in this acidic etchant [12]. Meanwhile, the impurities in the neighbourhood of these defects could also magnify the chemical etching re-

action. The dissolution phenomena in the aluminium induced by hydrofluoric acid usually starts after a relatively high immersion time (30–50 min) [12]. The addition of a small quantity of hydrofluoric acid to other acids allows the electrochemical dissolution of the alloy to be promoted. In addition, HF acid reacts with Si-rich precipitates, favouring a selective dissolution in its neighbouring area,

thus influencing the large corrosion phenomena induced by HCl acid solution. The selective dissolution favoured by HF, coupled with the wide and general action of HCl, could be considered responsible for the obtained coral-like structure.

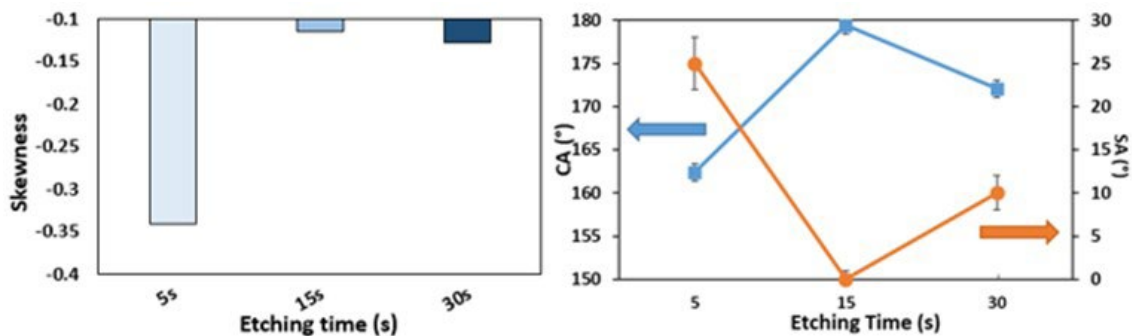


Fig.2 - Skewness parameters, Contact angle (CA) and sliding angle (SA) of etched samples.

In order to quantify the differences between the three etched surfaces and assess their relationship with the wettability behaviour of the aluminium alloy surfaces, the roughness parameters were calculated for Al surfaces after treatment.

An important parameter, Skewness (S_{sk}), was selected to evaluate the effect of the etching time on the surface morphologies. The skewness parameter, S_{sk} , is related to the degree of the symmetry of the variation in a profile about its mean line. S_{sk} near zero, if the distribution is quite symmetrical (equal repartition between peaks as valleys). A low negative S_{sk} value indicates that the height distribution is skewed above the mean plane and it is related to a profile with deep valleys such as porous structure.

In fact, the histogram of S_{sk} against the etching time evidenced a dependence between these parameters. Indeed, the sample etched for 15 seconds is characterized by the closest S_{sk} to zero indicating a quite symmetric distribution of peaks and valleys. However, at the lowest immersion time (5s), the etched surface is characterized by the lowest S_{sk} parameter indicating the presence of deep valleys. At the highest etching time (30s), a decrease of skewness value of about 12% was observed demonstrating that

the distribution of peaks and valleys on this surface are less homogenous than the sample etched for 15s.

In order to study the effect of the achieved morphologies on the wetting behaviour of the aluminium alloy samples, the water contact angles and the water sliding angles were measured (Fig. 2).

It is clear that superhydrophobicity was initially enhanced by increasing the etching time, and then reduced after an etching time of 30s. In particular, the highest CA (180°) and the lowest SA angles (0°) were obtained for the surface etched for 15s. Indeed, the CA rises by about 12%, from 161° to around 180° , and the SA decreases from 27° to around 0° degrees when the etching time increases from 5s to 15s min. While all the aluminium specimens are superhydrophobic with a CA higher than 150° , the difference in the wetting behaviour at increasing etching time is related to the diverse interactions of the as prepared surface with water (Cassie-Baxter or Wenzel states). In the Cassie-Baxter, the air-layer entrapped by the rough structure is able to significantly reduce the contact angle between the liquid and the surface, and thus the water droplet easily rolls off as on the case of the sample 15s. However, in the Wenzel state, the liquid droplet pene-

trates the surface grooves resulting in high adhesion and thus high sliding angle. Consequently, the portion of air trapped in the solid/water interface is the key factor that controls the CA and SA and thus the anti-wetting surface type.

Our results point out that a transition between Wenzel and Cassie-Baxter states can be controlled by modifying the etching time. The 5s sample is in intermediate state between Wenzel and Cassie-Baxter since the sliding angle is quite elevated (27°) indicating that the air layer is not continuous (air is only partially entrapped into the surface valleys). However, the 15s and 30s samples are Cassie-Baxter surfaces as indirectly identifiable by the low SA ($0 \leq SA \leq 10^\circ$) which is probably due to the regular and homogeneous roughness that enhance the formation of an almost continuous air film (Fig.2). This result is consistent with the literature. In fact, Li and Amirfazli demonstrated that the achievement of a high CA and a low SA

on a solid surface requires a hierarchical structure with a high air fraction [13]. When the etching time increases to 30s, the ordered structure starts to be lost which affect the air layer. Indeed, the air fraction trapped on the solid surface of the 30s sample surface is probably lower than the 15s sample resulting in lower CA (174°) and higher SA (10°) but it still enough to maintain the Cassie-Baxter state (Fig.2). Thus, the water repellence behaviour follows the same order of the Skewness parameter: The best behaviour was observed on the 15s sample surface having the highest S_{SK} followed by the 30s and then the 5s samples. Superhydrophobic surfaces with different water repellency behaviour were successfully elaborated. This reduction in the wettability of these surfaces may deeply affect their corrosion resistance.

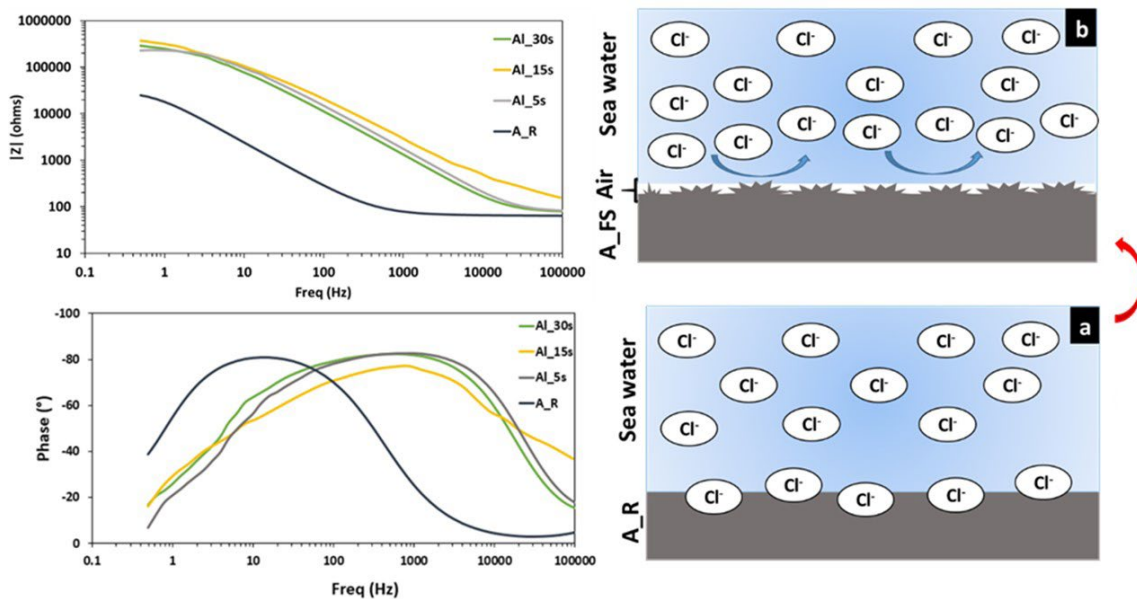


Fig.3 - EIS curves of as received aluminium alloy and the superhydrophobic surfaces in seawater at room temperature.

The ability of the superhydrophobic surfaces to protect the aluminium alloy from corrosion was evaluated by the electrochemical impedance spectroscopy (EIS). The EIS curves recorded for the as received aluminium alloy and superhydrophobic aluminium surfaces, having different CA and SA, in simulated seawater (3.5 wt% NaCl solution)

are presented in Fig.3.

At low frequencies, all impedance modulus curves exhibit a small plateau. The plateau in the as received sample spectrum is ascribed to the thin aluminium oxide surface ($\sim 2.5 \cdot 10^4 \Omega \cdot \text{cm}^2$ at 0.5 Hz). After the creation of superhydrophobic surfaces, an evident increase of impedance

magnitude in all the frequency range can be highlighted. Indeed, an increase of the $|Z|$ by more than one order of magnitude compared to the A_R sample was observed. The highest magnitude of impedance modulus, about $\sim 3 \cdot 10^5 \Omega \cdot \text{cm}^2$ at low frequency range, was observed for AL_15s which has the highest CA and the lowest SA.

By evaluating the phase plot, it is possible to identify apparently a single time constant for all batches. The as received sample, A_R, exhibits a peak in the phase angle at low frequency ($\sim 10^1$ Hz) that can be associated to the aluminium oxide layer. The EIS spectra of superhydrophobic samples are characterized by a wider phase peak at high frequencies. In fact, a time constant can be identified at high frequency ($\sim 10^3$ Hz), in correspondence of the phase peak. This trend is typical of the capacitive behaviour of external protective layers. In addition, the phase angle near to -90° indicates that this protective film provides a good barrier action. This behaviour can be ascribed to the coupled action of the surface texturing and silanization. The surface modification acts on shift of the peak at very high frequency, probably related to the formation of a protective layer of air. This air layer can work as the dielectric for a parallel plate capacitor that prevents the Cl^- from moving between the electrolyte and the aluminium surface. Indeed, the trapped air on the hierarchical rough surfaces of the superhydrophobic aluminium surfaces acts as an "air cushion" inhibiting the penetration of corrosive ions (Cl^-) and leading to an improved corrosion protection as shown in the Fig.3.b. Thus, these superhydrophobic surfaces enhances the corrosion resistance of the aluminum alloy.

CONCLUSIONS

Superhydrophobic surfaces were created on aluminium alloy by the coupling the chemical etching and the decrease of surface energy obtained by silane coating. The wettability state of these superhydrophobic surfaces varies with the etching time. In fact, the Cassie-Baxter state ($\text{CA} \approx 180^\circ$ and $\text{SA} \approx 0^\circ$) was achieved by a chemical etching for 15s. On the other hand, an intermediate state between Wenzel and Cassie-Baxter was obtained for the lowest etching time 5s. Thus, the wetting transitions from Wenzel to Cassie-Baxter can be controlled by modifying the etching time. The wetting state alteration is based on the distribution of the roughness peaks and valley. In addition, the as-modified aluminium surfaces revealed a good corrosion resistance behaviour in 3.5 wt% NaCl solution compared with the as received one and the best results were obtained on the Cassie-Baxter surfaces. Thus, a symmetric distribution of peaks and valleys is the key factor for obtaining the Cassie-Baxter state and thus for improving the superhydrophobicity and the corrosion behaviour of the aluminium alloy.

REFERENCES

- [1] L. Calabrese, E. Proverbio, A. Khaskhoussi, Superhydrophobic behaviour of modified AA6082 alloy surfaces, *Metall. Ital.* 111 (2019) 6–10.
- [2] A. Khaskhoussi, L. Calabrese, E. Proverbio, An Easy Approach for Obtaining Superhydrophobic Surfaces and their Applications, *Key Eng. Mater.* 813 (2019) 37–42. <https://doi.org/10.4028/www.scientific.net/KEM.813.37>.
- [3] B. Zhang, Q. Zhu, Y. Li, B. Hou, Facile fluorine-free one step fabrication of superhydrophobic aluminum surface towards self-cleaning and marine anticorrosion, *Chem. Eng. J.* 352 (2018) 625–633. <https://doi.org/10.1016/j.cej.2018.07.074>.
- [4] X. Wang, Y. Pan, X. Liu, H. Liu, N. Li, C. Liu, D.W. Schubert, C. Shen, Facile Fabrication of Superhydrophobic and Eco-Friendly Poly(lactic acid) Foam for Oil-Water Separation via Skin Peeling, *ACS Appl. Mater. Interfaces.* 11 (2019) 14362–14367. <https://doi.org/10.1021/acsami.9b02285>.
- [5] W. Li, Y. Zhan, S. Yu, Applications of superhydrophobic coatings in anti-icing: Theory, mechanisms, impact factors, challenges and perspectives, *Prog. Org. Coatings.* 152 (2021) 106117. <https://doi.org/10.1016/j.PORGCOAT.2020.106117>.

- [6] K. Vidal, E. Gómez, A.M. Goitandia, A. Angulo-Ibáñez, E. Aranzabe, The Synthesis of a Superhydrophobic and Thermal Stable Silica Coating via Sol-Gel Process, *Coatings* 2019, Vol. 9, Page 627. 9 (2019) 627. <https://doi.org/10.3390/COATINGS9100627>.
- [7] Q. Fan, X. Ji, Q. Lan, H. Zhang, Q. Li, S. Zhang, B. Yang, An anti-icing copper-based superhydrophobic layer prepared by one-step electrodeposition in both cathode and anode, *Colloids Surfaces A Physicochem. Eng. Asp.* 637 (2022). <https://doi.org/10.1016/j.colsurfa.2021.128220>.
- [8] R. Tan, H. Xie, J. She, J. Liang, H. He, J. Li, Z. Fan, B. Liu, A new approach to fabricate superhydrophobic and antibacterial low density isotropic pyrocarbon by using catalyst free chemical vapor deposition, *Carbon N. Y.* 145 (2019) 359–366. <https://doi.org/10.1016/j.carbon.2019.01.041>.
- [9] X. Su, H. Li, X. Lai, Z. Yang, Z. Chen, W. Wu, X. Zeng, Vacuum-assisted layer-by-layer superhydrophobic carbon nanotube films with electrothermal and photothermal effects for deicing and controllable manipulation, *J. Mater. Chem. A.* 6 (2018) 16910–16919. <https://doi.org/10.1039/C8TA05273E>.
- [10] P.D. Srivyas, M.S. Charoo, Application of Hybrid Aluminum Matrix Composite in Automotive Industry, *Mater. Today Proc.* 18 (2019) 3189–3200. <https://doi.org/10.1016/j.matpr.2019.07.195>.
- [11] A. KHASKHOUSI, L. CALABRESE, E. PROVERBIO, Effect of the Cassie Baxter-Wenzel behaviour transitions on the corrosion performances of AA6082 superhydrophobic surfaces, *Metall. Ital.* (2021) 15–21.
- [12] M.E. Straumanis, Y.N. Wang, The Rate and Mechanism of Dissolution of Purest Aluminum in Hydrofluoric Acid, *J. Electrochem. Soc.* 102 (1955) 370–381. <https://doi.org/10.1149/1.2430103>.
- [13] W. Li, A. Amirfazli, Microtextured superhydrophobic surfaces: A thermodynamic analysis, *Adv. Colloid Interface Sci.* 132 (2007) 51–68. <https://doi.org/10.1016/j.cis.2007.01.001>.

Fabbricazione di superfici superidrofobiche su lega di alluminio AA6082 mediante etching in soluzione HF/HCl per una maggiore protezione dalla corrosione

La sfida più importante nella cantieristica navale è la riduzione del peso delle strutture navali tradizionalmente realizzate in acciaio al fine di aumentarne la stabilità e la sicurezza. L'alluminio e le sue leghe sono potenziali materiali candidati grazie alla loro leggerezza e all'eccellente saldabilità. Tuttavia, le leghe di alluminio sono soggette a corrosione per vaiolatura in ambiente salino. Il controllo dell'idrorepellenza della superficie dell'alluminio può fornire una soluzione efficace per la protezione della stessa. Nel presente lavoro sono stati valutati l'effetto dell'etching chimico sulla morfologia della superficie e il comportamento dopo idrofobizzazione con un trattamento in soluzione base silanica. Sono stati considerati tempi di attacco diversi per ottimizzare l'effetto del trattamento. I risultati indicano che le superfici preparate hanno raggiunto il valore soglia di superidrofobicità (150°). Tuttavia, gli angoli di contatto e di scorrimento dipendono fortemente dal tempo di attacco. Le superfici superidrofobiche ottimizzate hanno mostrato una maggiore protezione dalla corrosione rispetto all'AA6082 tal quale in acqua di mare simulata.

PAROLE CHIAVE: SUPER-IDROFOBICITA'; LEGA DI ALLUMINIO; CORROSIONE; ATTACCO CHIMICO.

TORNA ALL'INDICE >